Electronic Supplementary Material (ESI) for Journal of Materials Chemistry C.

Unconventional dihydrogen-bond interaction induced cyanide-bridged chiral nano-sized magnetic molecular wheel: synthesis, crystal structure and systematically theoretical magnetism investigation

Daopeng Zhang,[a,+] Joan Cano,[b,+] Wenlong Lan,[a] Hui Liu,[a,*] Fenggang Sun,[a] Yunhui Dong,[a] Zhen Zhou,[a] Lu Yang,[a] Qingyun Liu,[d] and Jianzhuang Jiang[c,*]

[a]College of Chemical and Chemical Engineering, Shandong University of Technology, Zibo 255049, PR China.

[b]Institut de Ciència Molecular (ICMol), Universitat de València, 46980 Paterna, València

[c]Department of Chemistry, University of Science and Technology Beijing, Beijing 100083, China

[d]College of Chemical and Environmental Engineering, Shandong University of Science and Technology, Qingdao 266510, PR China.

*E-mail: dpzhang73@126.com, jianzhuang@ustb.edu.cn

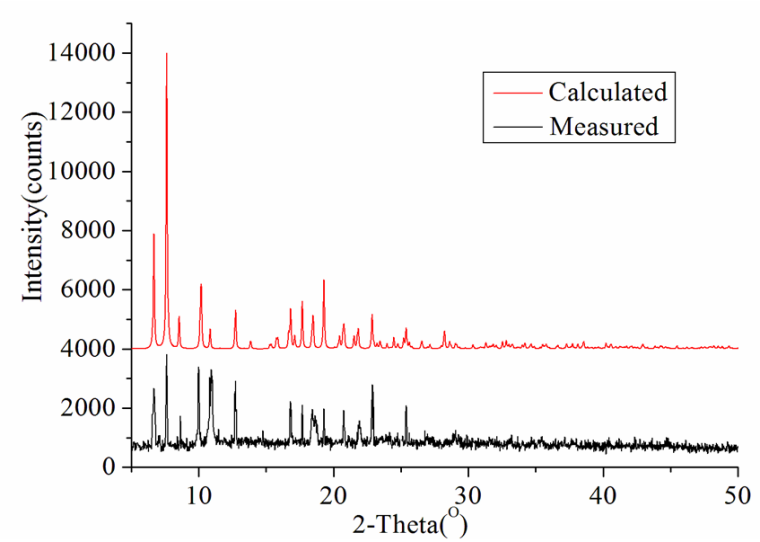

Figure S1. The powder X-ray diffraction pattern of the complex **1**.

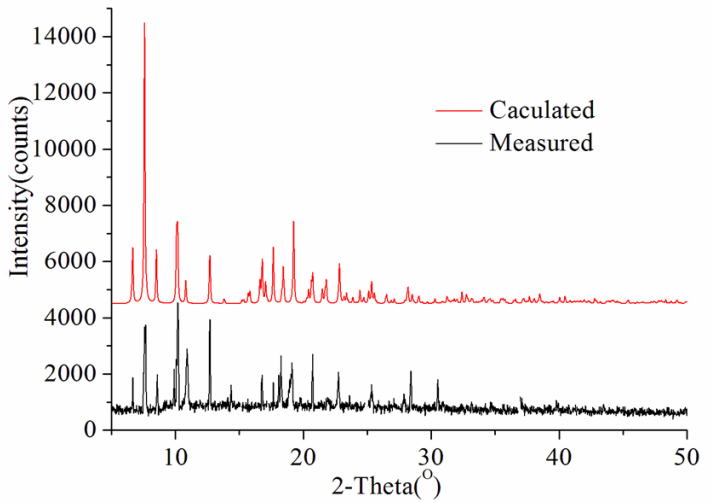

Figure S2. The powder X-ray diffraction pattern of the complex **2**.

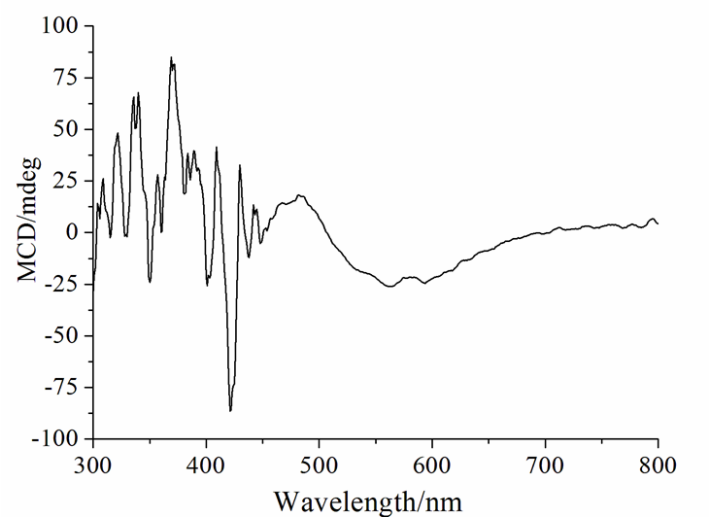

Figure S3. The MCD spectra of the complex **1**.

Table S1. The seclected bond lengths and angles of the complex **1**.

1			
Ru(1)-C(1)	2.076(17)	Ru(2)-C(39)	2.070(2)
Ru(1)-C(2)	2.06(2)	Ru(2)-C(40)	2.040(2)
Ru(1)-N(3)	1.99(2)	Ru(2)-N(9)	2.027(15)
Ru(1)-N(4)	1.938(18)	Ru(2)-N(10)	2.012(18)
Ru(1)-O(1)	2.029(14)	Ru(2)-O(5)	2.058(12)
Ru(1)-O(2)	1.951(12)	Ru(2)-O(6)	2.008(13)
Mn(1)-N(1)	2.240(18)	Mn(2)-N(2)	2.276(16)
Mn(1)-N(5)	2.029(17)	Mn(2)-N(8)	2.265(18)
Mn(1)-N(6)	2.026(16)	Mn(2)-N(11)	1.943(15)
Mn(1)-N(7)	2.337(15)	Mn(2)-N(12)	1.965(14)
Mn(1)-O(3)	1.869(14)	Mn(2)-O(7)	1.906(12)
Mn(1)-O(4)	1.850(14)	Mn(2)-O(8)	1.933(15)
C(1)-N(1)-Mn(1)	163.2(16)	C(2)#3-N(2)-Mn(2)	146.4(15)
C(39)-N(7)-Mn(1)	139.5(14)	C(40)-N(8)-Mn(2)	164.4(17)
N(1)-C(1)-Ru(1)	177.7(17)	N(7)-C(39)-Ru(2)	175.4(16)
N(2)#4-C(2)-Ru(1)	175.0(17)	N(8)-C(40)-Ru(2)	170.5(17)

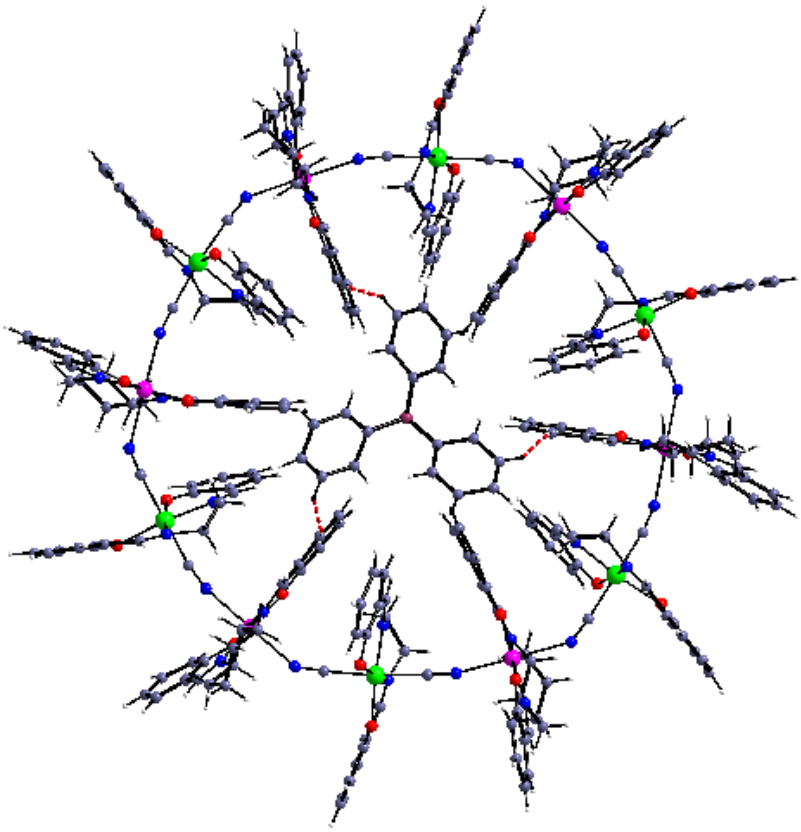

Figure S4. The dihydrogen-bond supramolecular diagram between the macrocycle entity and the co-crystallized PPh_3 molecule.

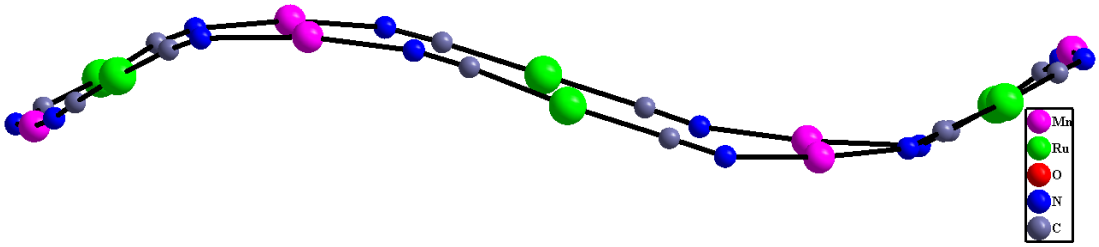

Figure S5. The cyclohexane chair-like conformation of the macrocyclic skeleton of the complex **1**.

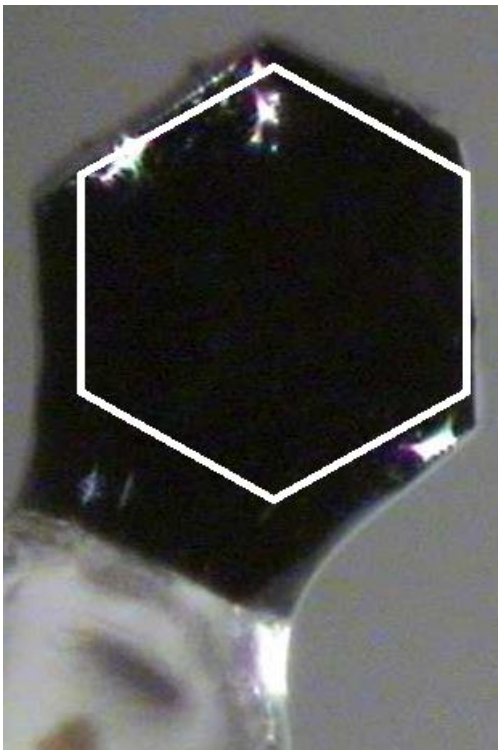

Figure S6. The regular hexagonal block-like dark-brown single crystal of the complex **1**.

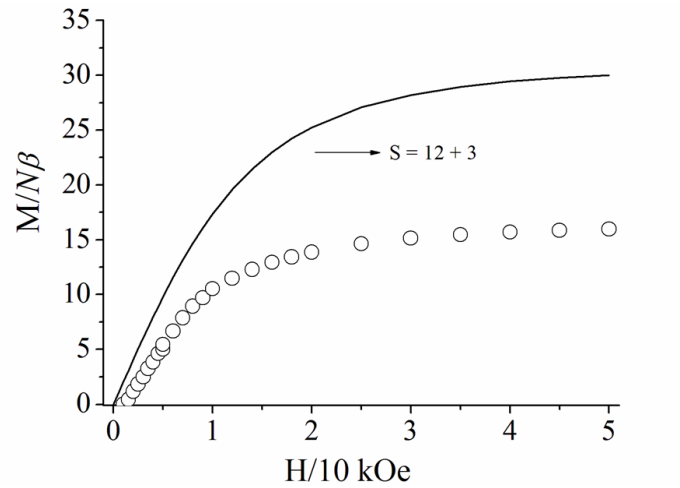

Figure S7. The field dependence of magnetization at 2 K of the complex **1**. The calculated curve are with six pairs of Mn(III)-Ru(II) units based-on S_{Mn}= 2, S_{Ru} = 1/2.

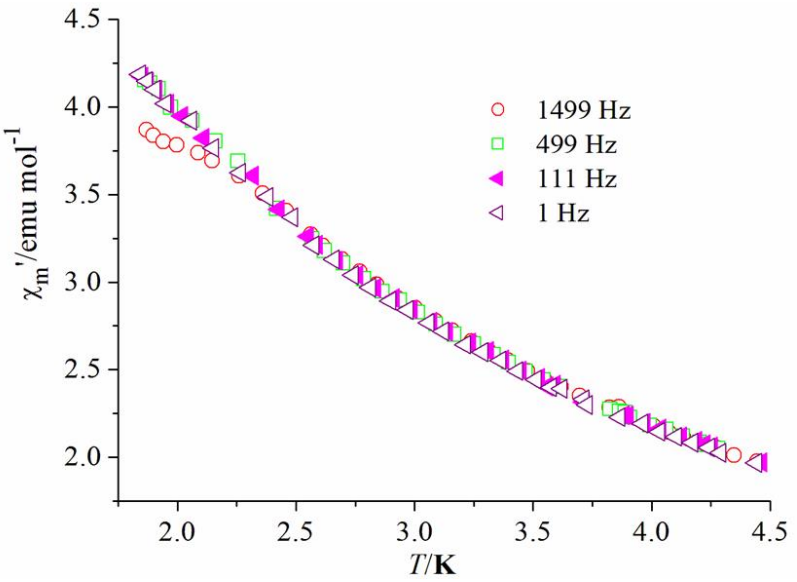

Figure S8. Frequency dependence of the in-phase χ_M' vs. T for the complex **1**.

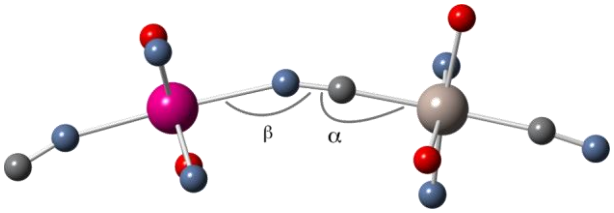

Figure S9. Simplified view of a {RuMn} unity showing the more important geometrical parameters [the Ru–C≡N angle (α) and the Mn–N≡C angle (β)] influencing on the magnetic coupling between Ru^{III} and Mn^{III} ions (see Table 2 and text). Color code: Ru (red-grey), Mn (purple), C (grey), N (blue) and O (red).

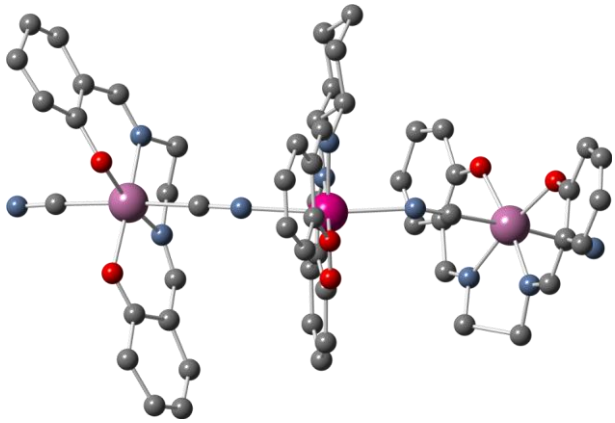

Figure S10. View of the molecular model used to establish a magneto-structural correlation with the β bond angle displayed in Figure S9. For clarity, hydrogen atoms were hidden. Color code: Mn(purple), C (grey), N (blue), O (red) and In (pale purple).

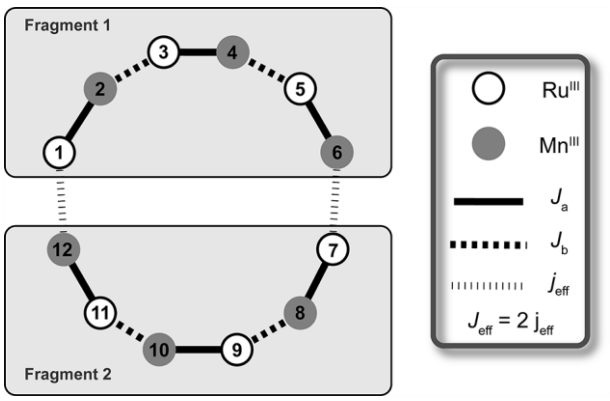

Figure S11. Fragmentation of the scheme of the topology of the spin-spin exchange interactions shown in Figure 6 under the approach based on effective spin momenta and couplings.

The magnetic fitting for $\chi_M T$ was carried out using the approximate 1D model with the mean-field approximation included based-on the Hamiltonian $H = -J\sum_{i=0}^{N} S_i S_{i+1}$, in which the J value is the intramolecular magnetic coupling between the Ru(III) ion and Mn(III) ion through the cyanide bridge. To take into account the effects other than the intramolecular magnetic coupling, such as zfs and intermolecular magnetic coupling), the mean-field approximation (*zJ'*) has been employed. Equations used to fit are as follows. Only one g value was used for simplification and the best-fit parameters obtained are J = -7.16 cm^{-1}, g = 1.99, zj' = 0.91 cm^{-1} and $R = (\sum(\chi_{calcd} - \chi_{obsd})^2)/\chi_{obsd}^2 = 3.9 \times 10^{-4}$.

$$\chi^{chain} = \frac{2N\beta^2}{3kT}\left[M^2\frac{1+P}{1-P} + (\delta M)^2\frac{1-P}{1+P}\right]$$

$$P = \coth(J_{eff} / kT) - kT / J_{eff}$$

$$M = [g_{Mn}[S_{Mn}(S_{Mn}+1)]^{1/2} + g_{Ru}[S_{Ru}(S_{Ru}+1)]^{1/2}]/2$$

$$\delta M = [g_{Mn}[S_{Mn}(S_{Mn}+1)]^{1/2} - g_{Ru}[S_{Ru}(S_{Ru}+1)]^{1/2}]/2$$

$$J_{eff} = J[S_{Mn}(S_{Mn}+1)S_{Ru}(S_{Ru}+1)]^{1/2}$$

$$\chi_M = \frac{\chi_{chain}}{1 - \chi_{chain}(2zJ'/Ng^2\beta^2)}$$

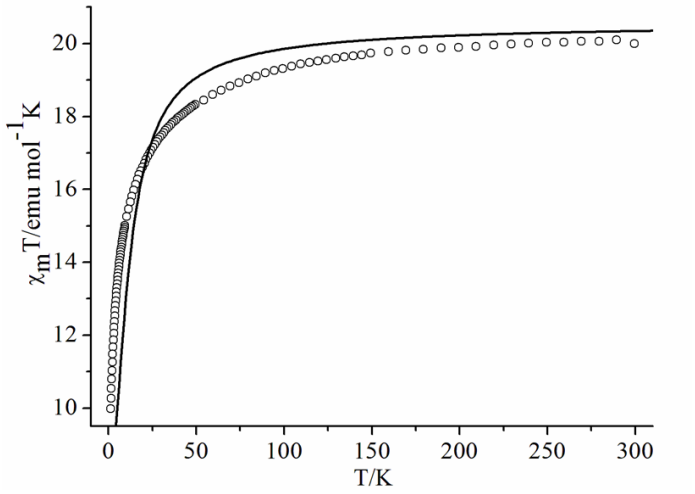

Figure S12. The magnetic fitting for $\chi_m T$ using the approximate 1D model.